Journal of Non-Crystalline Solids xxx (xxxx) xxx–xxx

Contents lists available at ScienceDirect

Journal of Non-Crystalline Solids

journal homepage: www.elsevier.com/locate/jnoncrysol

# Permanent densification of amorphous zinc oxide under pressure: A first principles study

Duygu Tahaoğlu, Murat Durandurdu*

*Department of Materials Science & Nanotechnology Engineering, Abdullah Gül University, Kayseri 38080, Turkey*

ARTICLE INFO

*Keywords:*
ZnO
Amorphous
Densification
Phase transformation

ABSTRACT

Ab initio simulations within a generalized gradient approximation are carried out to investigate the densification mechanism of amorphous zinc oxide (a-ZnO) under hydrostatic pressure. In contrast to the crystalline ZnO, the densification of a-ZnO is found to proceed gradually and is associated with a structural modification from a low density amorphous state to a high density amorphous state. Accompanied by the phase transformation, the mean coordination number increases from ~4.0 to ~5.5. The high-density amorphous form of ZnO has a local structure, partially comparable with that of the rocksalt type ZnO crystal and presents a semiconducting behavior. The phase change is irreversible because upon pressure release, an amorphous model largely consisting of fivefold coordination is recovered. The decompressed model can be, therefore, classified as an intermediate phase between the wurtzite-like and the rocksalt-like amorphous configurations.

## 1. Introduction

Zinc oxide (ZnO) has been drawing the attention of researchers for decades, particularly as a semiconductor material due to its low cost, high abundancy and non-toxic nature [1] besides its wide direct bandgap (~3.37 eV at room temperature) makes this material a good alternative for the optoelectronic devices of short-wavelength [2]. Its piezoelectricity, good chemical properties in terms of stability and catalytic activity, optical and electrical properties also make ZnO a convenient candidate for other application areas such as micro sensors, transparent conductive oxides, catalytic use, and space applications [3,4]. In virtue of all these features, ZnO is an extensively studied material for the last decades, with a history going back to 1920s. Major part of all these studies involves the investigation of its physical, mechanical and electronic properties.

ZnO, a member of II–VI group of semiconductors, has a tendency to crystallize in the wurtzite (WZ) structure. Under hydrostatic compression, a structural phase transformation from the WZ crystal to a rocksalt (RS) structure occurs at around 10 GPa [5].

Some advantageous features of amorphous materials such as permitting economic manufacturing in large dimensions and having competitive characteristics with the crystalline ones bring a new point of view to the oxide semiconductor materials market [1]. Even though high quality ZnO crystals can be obtained in bulk form [6], the growth process of the crystalline ZnO films requires high temperatures around 500–800 °C, which is an important drawback against the amorphous ZnO (a-ZnO) [2]. Higher cost to produce crystalline materials is also another factor to direct interest of the researchers on amorphous materials [6].

Although the properties, manufacturing methods and application fields of the crystalline form of the ZnO have been studied comprehensively, there are limited studies on the synthesis and characterization of a-ZnO [2,7,8] and thus there is a little known and a great unexplored space for a-ZnO in terms of its structure and properties.

In this study, the effects of high pressure treatment on the structure of a-ZnO are for the first time investigated using a constant pressure ab initio approach and a gradual irreversible amorphous-to-amorphous phase change is proposed for it.

## 2. Computational method

The initial a-ZnO model was generated by Drabold's group from the liquid state using a first principles molecular dynamics technique [9]. The amorphous model consists of 128 atoms (64 Zn atoms and 64 O atoms). For the crystalline ZnO, a supercell having 108 atoms was constracted. Both structures at zero pressure were optimized using the ab initio code SIESTA [10] within the generalized gradient approximation of Perdew-Burke-Ernzerhof (PBE) [11]. The Troullier and Martins scheme was used to contract pseudopotentials [12]. The double zeta plus polarized orbitals were chosen for the calculations. The simulations were executed within the isoenthalpic-isobaric (NPH) ensemble. The pressure optimization was achieved by the Parrinello-

* Corresponding author.
*E-mail address:* murat.durandurdu@agu.edu.tr (M. Durandurdu).

http://dx.doi.org/10.1016/j.jnoncrysol.2017.10.016
Received 19 June 2017; Received in revised form 26 September 2017; Accepted 12 October 2017

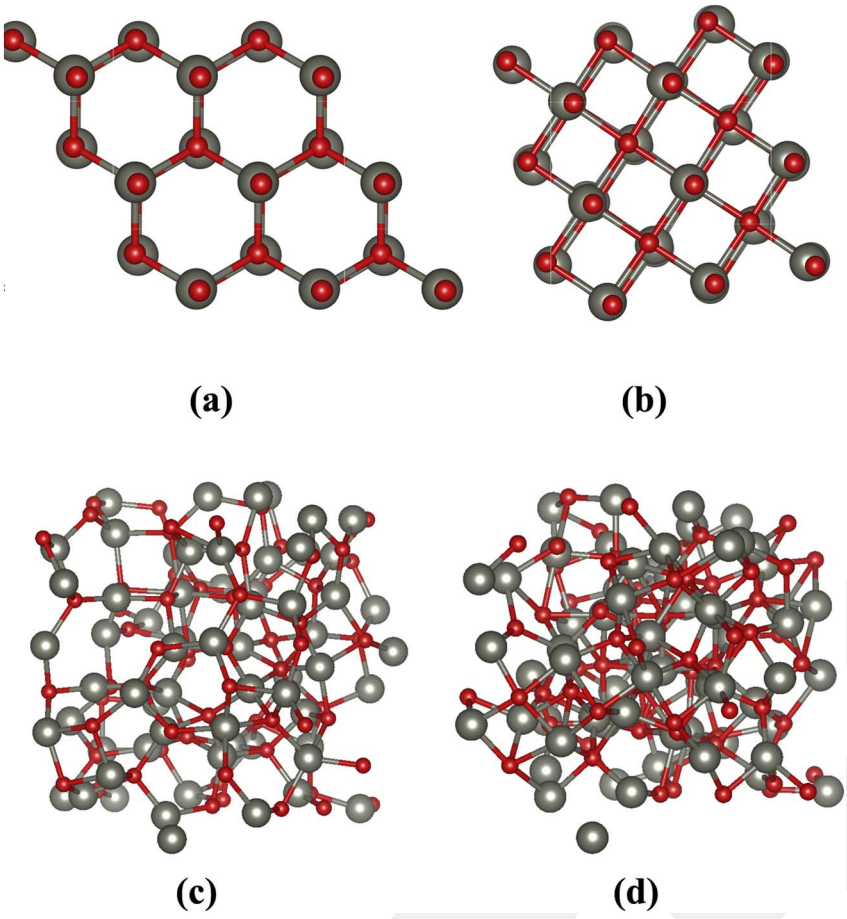


**Fig. 1.** Ball stick representation of (a) the WZ crystal (b) the RS structure obtained at 35 GPa, (c) the initial a-ZnO model and (d) the high coordinated amorphous phase at 54 GPa.

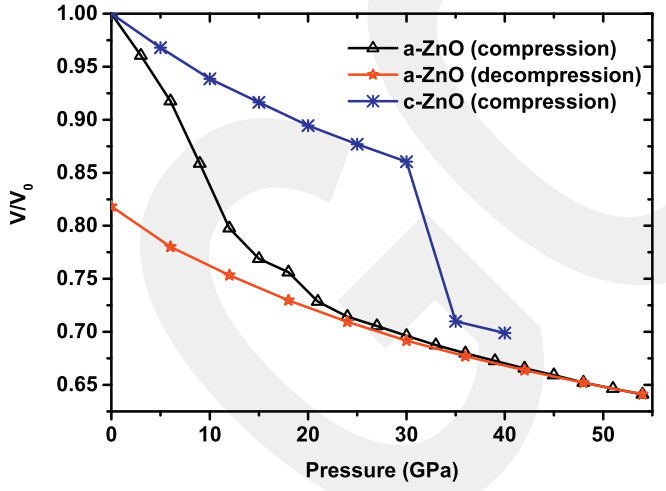


**Fig. 2.** Pressure volume relation of the crystalline phase under pressure and of a-ZnO on compression and decompression.

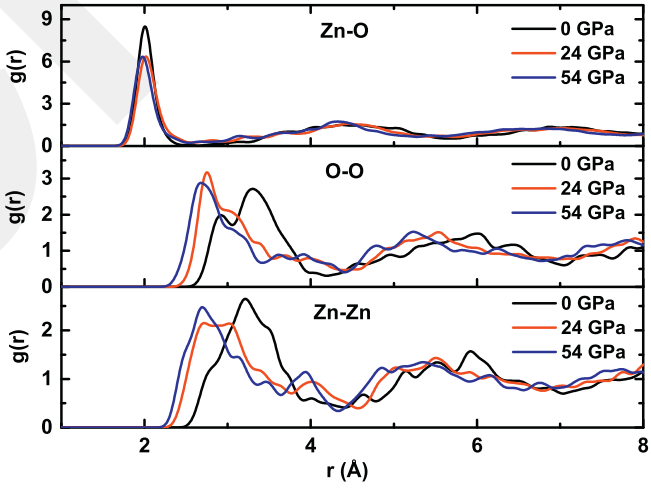


**Fig. 3.** Partial pair distribution functions at some pressures.

Rahman method [13]. The external pressure was gradually applied up to 54 GPa for a-ZnO using an increment of 3 GPa and up to 45 GPa using an increment of 5 GPa for the crystalline ZnO. The VESTA [14] program was used to visualize the structures.

## 3. Results

In order to verify that the parameters (pseudopotentials, basis, etc.) chosen in the simulations are trustworthy to investigate the high-pressure behavior of a-ZnO, first we test them for the WZ crystal. As shown in Figs. 1 and 2, a phase transformation from the WZ crystal to a RS crystal at a theoretical pressure of 35 GPa with a first order nature is successfully observed throughout the simulation. This observation shows that the parameters used in the present work are good enough to capture the experimentally revealed phase transformation and hence they can be securely applied to a-ZnO. It should be noted here that the phase transformation from the WZ crystal to a RS structure in the simulation happens at an exaggerated critical pressure of 35 GPa, relative to the experimental value of 10 GPa. The overestimation in transition pressures is usually perceived in the Parrinello-Rahman dynamics [15,16] and can be linked to some limitations such as time scale, no

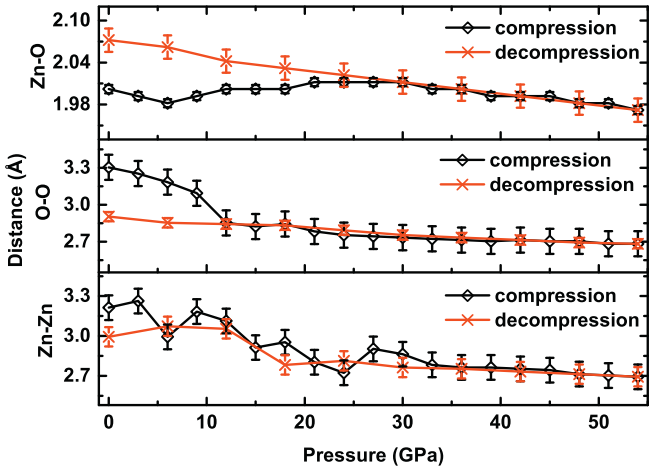


**Fig. 4.** Variation of Zn−O, Zn−Zn and O−O distances under pressure.

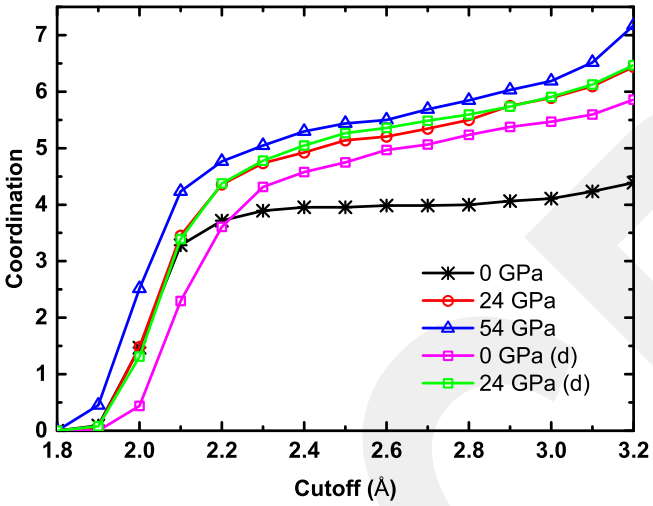


**Fig. 5.** Mean coordination number as a function of cutoff radius.

surface effects etc. in simulations [15,16]. Consequently any phase transformation that will be exposed for a-ZnO in the present work will be expected to appear/start at a lower pressure in experiments.

The alteration of volume of a-ZnO during the compression and decompression processes is also provided in Fig. 2. Up to 21 GPa, a rapid decrease (about 27%) in the volume is observed, which specifies major structural rearrangements in the amorphous network under pressure. After 21 GPa, the pressure volume curve exhibits a change in slope and the compression of the amorphous model becomes much slower. The change in the slope can be inferred as an indication of a phase transformation in the system. Upon decompression, the path followed from 54 GPa is reversed up to 21 GPa. After that point, it shows a hysteresis and a structure being ~18% denser than initial amorphous configuration is recovered, specifying a pressure-induced permanent densification in a-ZnO.

In order to distinguish the structural features and to expose the essential rearmaments in a-ZnO at the atomistic level at ambient and high pressures, the pair distribution function analysis is carried out. Fig. 3 illustrates the partial pair distribution functions and their variations at some specific pressures. The inexistence of long-range correlations reveals that the structure is not rearranged itself into a crystalline state up to the highest pressure of 54 GPa applied in the present simulation and it undergoes an amorphous-to-amorphous phase transformation (see Fig. 2).

To have a further insight on the local structural changes in the model at each applied pressure, we study the variation of Zn−O, Zn−Zn and O−O correlations and show them in Fig. 4. At zero pressure, the first peak of the Zn−O, Zn−Zn and O−O correlations is located at ~2.0 Å, 3.21 Å and 3.30 Å, respectively. They are reasonably comparable with the experimental predictions of 1.9767, 3.2138 and 3.2138 Å produced in the WZ phase [17]. This finding suggests that the initial amorphous structure is locally close to the WZ crystal and is free from chemical disorder, e.g., no homopolar (wrong) bonds. With the application of pressure, the Zn−O bond length rises up to 21 GPa, remains unaffected between 21 GPa and 30 GPa, and then progressively declines. Upon pressure release, the Zn−O bond distance gradually increases and has a value of 2.07 Å at ambient pressure, which is slightly longer than the mean Zn−O bond length (~2.0 Å) of the uncompressed model. The Zn−Zn and O−O separations, on the other hand, show a naive behavior and have a tendency to decrease gradually with increasing pressure. On decompression, as seen from Fig. 4, however, their original values are not recovered. From the pair distribution function analysis, we can also perceive that the model remains chemically ordered during the compression and decompression procedures.

The pressure-induced amorphous-to-amorphous phase transformations in open structured tetrahedrally coordinated materials are generally traced by the change in the mean total or partial coordination numbers. Therefore we next estimate them using the first minimum of the Zn−O correlation as a cutoff radius. Yet as the applied pressure is increased, we find no a well-defined first minimum in the Zn−O distribution. In order to accurately estimate the coordination number, we analyze it as a function of cutoff radius and show it in Fig. 5 (for clarity a few of them are shown in the figure). The coordination number first increases drastically and beyond a certain distance of about 2.2 Å, the change in the coordination number becomes much slower or null. For larger cutoff radii (about 2.5–2.6 Å for compressed and decompressed models) we perceive a small but noticeable change in the curve slope again and the coordination increase develops slightly faster. For the pre-compressed model, beyond 2.3 Å we notice a clear flat region that allows us easily to define a precise cutoff radius and hence the coordination number(s). During the compression and decompression processes, on the other hand, such a clear flat region is not easily accessible in the coordination-cutoff radius curve and hence the determination of the cutoff radii becomes rather challenging. For these cases, we choose a point (just below 2.6 Å) at which the second change in the slope of the coordination-cutoff radius curve is observed. Since the coordination numbers are very sensitive to the cutoff radius used, some uncertainties are expected for the values determined for them. The average coordination of the original a-ZnO material is ~4.0 and with the application of pressure, it slowly increases and reaches a value of ~5.5 beyond 36 GPa as shown in Fig. 5. Upon decompression, the mean coordination number remains almost null with a small fluctuation up to 5 GPa and has a value of 5.06 at zero-pressure, meaning that the high pressure induced configurations are persevered in the system and the amorphous-to-amorphous phase change is not reversible for a-ZnO.

To have detailed information about the microstructure of the model, we also investigate the coordination distribution of Zn and O atoms as a function of pressure and present them in Fig. 6 as well. At atmospheric pressure, the model essentially has the tetrahedral coordination with a frequency of more than 83%. It also has some undercoordinated (threefold ~ 11%) and overcoordinated (fivefold ~ 5%) motifs. As the applied pressure is increased, the number of tetrahedral coordination drastically decreases and becomes negligibly small beyond 36 GPa, while the fivefold coordination enormously increases between 3 GPa and 12 GPa for O atoms and between 3 GPa and 21 GPa for Zn atom. The fraction of the sixfold coordination becomes fairly visible beyond 12 GPa and rises gradually at high pressures. Beyond 36 GPa, the model has predominantly fivefold (~44%) and sixfold (~48%) configurations. Sevenfold coordinated arrangements that mostly occur around O atoms with a fraction of 5% also arise in the model above 36 GPa. The decompressed amorphous model consists of fivefold (82%) and sixfold

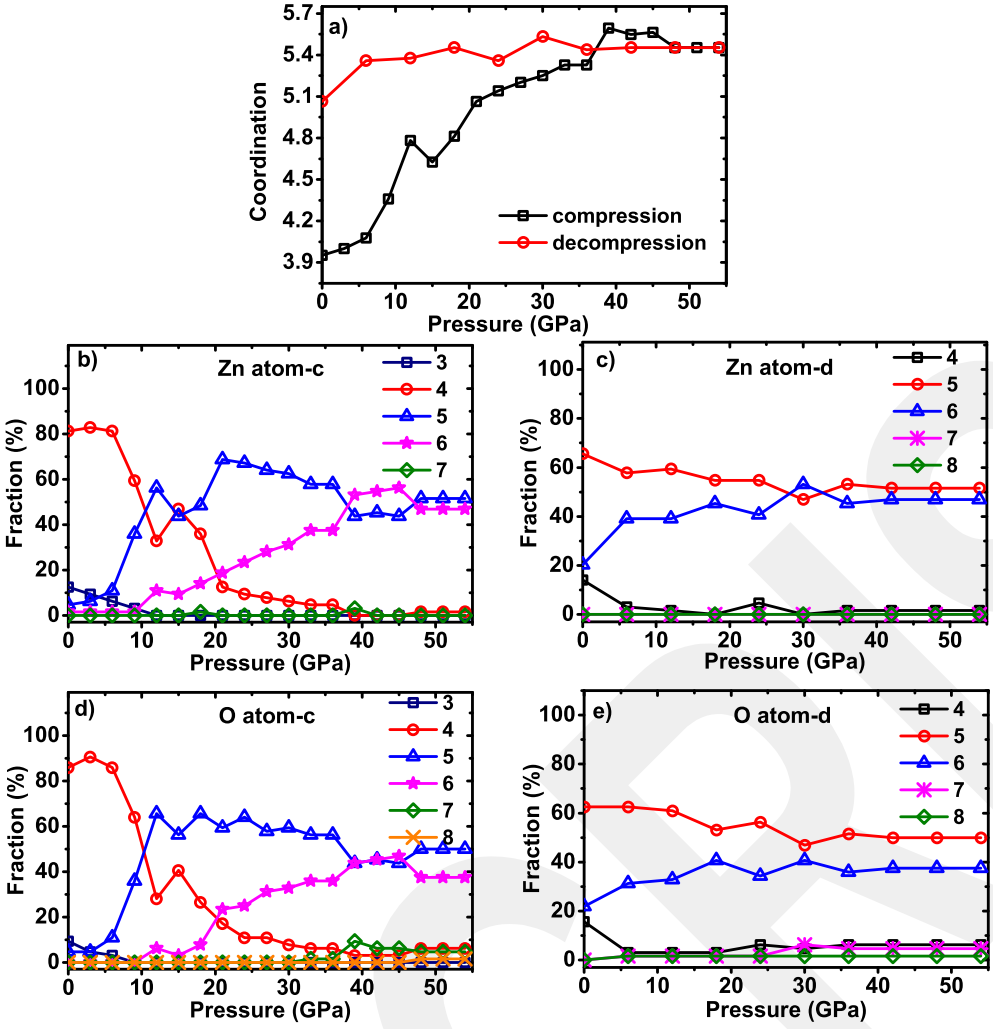


**Fig. 6.** (a) Variation of mean coordination number on compression and decompression. Coordination distribution of (b) Zn and (d) O atoms on compression and (c) Zn and (e) O atoms upon decompression.

(27%) coordination and has only 19% tetrahedral coordination. Consequently it can be classified as an intermediate state between the WZ-like and the RS-like amorphous phases.

The sixfold and fivefold configurations formed at high pressure correspond to ideal/deformed octahedrons and incomplete octahedrons, respectively as shown in Fig. 7. Therefore it is concluded that the short-range order of the high coordinated amorphous structure and the decompressed network is *partially* similar to the local structure of the RS phase.

To see how the electronic structure of the amorphous model and the crystalline ZnO changes under pressure, we compute the electronic eigenvalues and specifically focus on the variation of the HOMO-LUMO band gap energy under hydrostatic pressure as shown in Fig. 8. The HOMO-LUMO band gap energy of the a-ZnO model and the crystal is estimated to be 0.74 eV and 0.85 eV, respectively, fairly smaller than the experimental results of 1.60 eV [18] (amorphous) and 3.37 eV (crystal) due to the shortcoming of the DFT-GGA calculations. For the crystalline phase, the band bap increases gradually with increasing pressure and accompanied by the WZ-to-RS phase transformation, it suddenly jumps to a larger value. On the other hand, the HOMO-LUMO band gap fluctuates up to 27 GPa for a-ZnO. After this pressure, it gradually increases. The most important conclusion that can be inferred from the electronic structure calculations is that a-ZnO does not undergo the semiconductor-to-metal phase transformation, similar to the crystalline ZnO.

## 4. Discussion

We show, for the first time, the existence of an amorphous-to-amorphous phase transformation in ZnO under pressure, similar to what has been proposed in most tetrahedrally coordinated amorphous materials. Since the coordination modification takes place in a broad pressure range, the phase transformation of ZnO is classified as a gradual phase transformation. The formation of octahedrons-like and incomplete octahedrons-like configurations can be interpreted as a tendency of this material to attain a local structure similar to that of RS phase. This phase transformation is irreversible because the original density is not recovered and the high-pressure configurations (fivefold and sixfold) are mostly retained after full pressure release.

We can see two essential distinctions regarding the pressure induced phase transformation in the WZ-ZnO and a-ZnO. 1) The phase change is sharp (first-order) in the WZ-ZnO while it is gradual in a-ZnO. Indeed the different equation of state presented in these two forms is related to the disorder nature of a-ZnO, which allows the formation of a gradual coordination modification and a phase transformation in contrast to the crystal in which the phase transformation takes place homogeneously across entire supercell to reserve the transition symmetry. 2) The WZ-to-RS phase transformation in ZnO is reversible [19,20] (in some studies, the RS phase was found to be partially quenchable [21–23]) while the phase change in a-ZnO is irreversible. Our simulation suggests that the local structure of ZnO might play a key role for determining the nature of phase transformation and hence the observation of partially quenchable RS phase in experiments might be associated with some

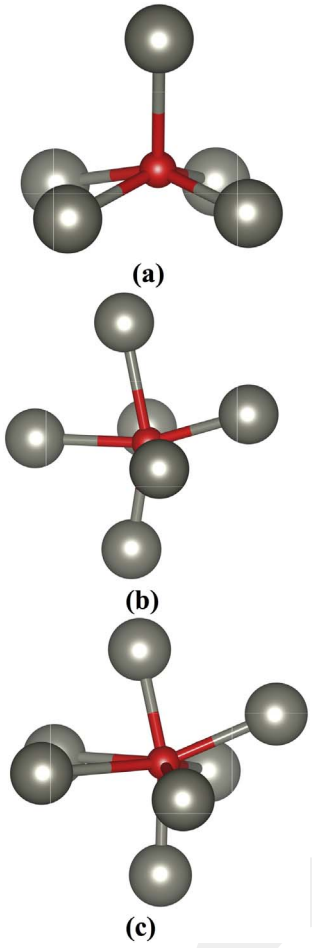


**Fig. 7.** Fivefold, sixfold and sevenfold coordinated configurations formed at high pressures.

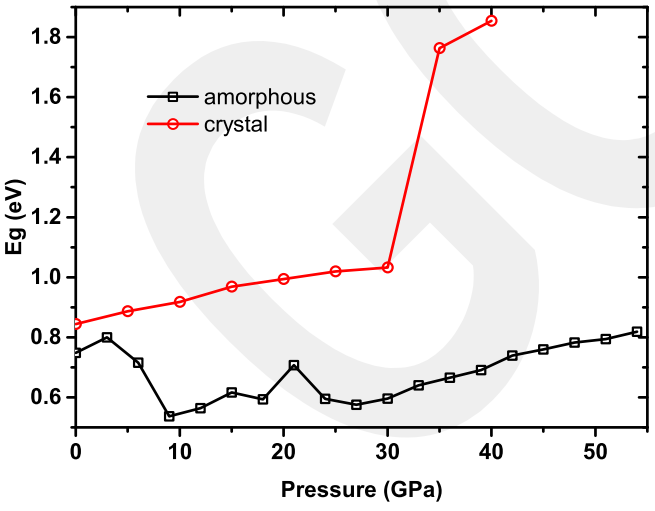


**Fig. 8.** Variation of the HOMO-LUMO band gap under pressure.

structural defects (disorders) existed in the compressed samples.

It is believed that the quenchable RS phase can yield new technological applications of ZnO [24,25]. Our decompressed model is indeed locally an intermediate state between the WZ-like and the RS-like amorphous phases since it predominantly consists of fivefold coordinated configurations. Therefore the observation of such an intermediate amorphous phase might lead to a new direction in the study of ZnO.

Finally we need to point out here that pressurization/depressurization in MD simulations occurs with very fast rates relative to experiments because of rather short time scales used in the simulations. Yet in spite of very fast compression/decompression rates, the nature of phase transformations (reversible/irreversible and gradual/first order) in different amorphous systems, comparable with experiments, was successfully captured in our earlier studies. Nonetheless the decompressed amorphous system of ZnO can be a frozen state due to the fast decompression rate. Therefore an experimental investigation is desirable to clarify this issue.

## 5. Conclusions

We investigate the structural modification of a-ZnO under pressure by means of an ab initio technique and find that a-ZnO exhibits a different densification mechanism compared to the crystalline ZnO phase. Namely, the pressure-induced phase transformation in a-ZnO proceeds gradually in contrast to the first order phase transformation in the crystal and is associated with a change from a low density amorphous state having an average coordination number of ~4.0 to a high density amorphous phase with a mean coordination number of ~5.5. The local structure of the high density amorphous phase is partially close to that of the RS structure. Upon pressure release, the high-density amorphous structure does not transform back to the original state. Instead it transforms to an intermediate state between the WZ-like and the RS-like amorphous phases, suggesting an irreversible phase transformation in a-ZnO. The electronic structure calculations reveal that a-ZnO remains semiconducting during the compression and decompression processes.

## Acknowledgements

We thank Prof. D. A. Drabold for providing us the initial a-ZnO model. This work was supported by the Abdullah Gül University Support Foundation. The calculations were carried out at HPCC at the Abdullah Gül University.

## References

[1] J.F. Wager, et al., An amorphous oxide semiconductor thin-film transistor route to oxide electronics, Curr. Opin. Solid State Mater. Sci. 18 (2) (2014) 53–61.
[2] J.M. Khoshman, M.E. Kordesch, Optical constants and band edge of amorphous zinc oxide thin films, Thin Solid Films 515 (18) (2007) 7393–7399.
[3] F. Claeyssens, et al., Growth of ZnO thin films - experiment and theory, J. Mater. Chem. 15 (1) (2005) 139–148.
[4] P. Nunes, et al., Effect of different dopant elements on the properties of ZnO thin films, Vacuum 64 (3–4) (2002) 281–285.
[5] U. Ozgur, et al., A comprehensive review of ZnO materials and devices, J. Appl. Phys. 98 (4) (2005).
[6] K.H. Lin, et al., Observation of the amorphous zinc oxide recrystalline process by molecular dynamics simulation, J. Appl. Phys. 113 (7) (2013).
[7] R. Theissmann, et al., High performance low temperature solution-processed zinc oxide thin film transistor, Thin Solid Films 519 (16) (2011) 5623–5628.
[8] A. Zawadzka, et al., Transparent amorphous zinc oxide thin films for NLO applications, Opt. Mater. 37 (2014) 327–337.
[9] A. Pandey, H. Scherich, D.A. Drabold, Density functional theory model of amorphous zinc oxide (a-ZnO) and a-X(0.375)Z(0.625)O (X = Al, Ga and In), J. Non-Cryst. Solids 455 (2017) 98–101.
[10] J.M. Soler, et al., The SIESTA method for ab initio order-N materials simulation, J. Phys. Condens. Matter 14 (11) (2002) 2745–2779.
[11] J.P. Perdew, K. Burke, M. Ernzerhof, Generalized gradient approximation made simple, Phys. Rev. Lett. 77 (18) (1996) 3865–3868.
[12] N. Troullier, J.L. Martins, Efficient pseudopotentials for plane-wave calculations, Phys. Rev. B 43 (3) (1991) 1993–2006.
[13] M. Parrinello, A. Rahman, Polymorphic transitions in single-crystals - a new molecular-dynamics method, J. Appl. Phys. 52 (12) (1981) 7182–7190.
[14] K. Momma, F. Izumi, VESTA 3 for three-dimensional visualization of crystal, volumetric and morphology data, J. Appl. Crystallogr. 44 (2011) 1272–1276.
[15] K. Mizushima, S. Yip, E. Kaxiras, Ideal crystal stability and pressure-induced phase-transition in silicon, Phys. Rev. B 50 (20) (1994) 14952–14959.
[16] R. Martonak, A. Laio, M. Parrinello, Predicting crystal structures: the Parrinello-Rahman method revisited, Phys. Rev. Lett. 90 (7) (2003).
[17] U. Seetawan, et al., Effect of calcinations temperature on crystallography and nanoparticles in ZnO disk, Mater. Sci. Appl. 2 (2011) 1302–1306.
[18] D. Schmeisser, et al., Electronic structure of amorphous ZnO films, Phys. Status

Solidi C 11 (9–10) (2014) 1476–1480.
[19] F. Decremps, et al., Local structure of condensed zinc oxide, Phys. Rev. B 68 (10) (2003).
[20] S. Desgreniers, High-density phases of ZnO: structural and compressive parameters, Phys. Rev. B 58 (21) (1998) 14102–14105.
[21] L. Gerward, J.S. Olsen, The high-pressure phase of zincite, J. Synchrotron Radiat. 2 (1995) 233–235.
[22] H.Z. Liu, et al., Rietveld refinement study of the pressure dependence of the internal structural parameter u in the wurtzite phase of ZnO, Phys. Rev. B 71 (21) (2005).
[23] J.M. Recio, et al., Compressibility of the high-pressure rocksalt phase of ZnO, Phys. Rev. B 58 (14) (1998) 8949–8954.
[24] F. Decremps, et al., Trapping of cubic ZnO nanocrystallites at ambient conditions, Appl. Phys. Lett. 81 (25) (2002) 4820–4822.
[25] H.Z. Liu, J.S. Tse, H.K. Mao, Stability of rocksalt phase of zinc oxide under strong compression: synchrotron X-ray diffraction experiments and first-principles calculation studies, J. Appl. Phys. 100 (9) (2006).